Detecting population continuity and ghost admixture among ancient genomes

Authors:
James McKenna, Carolina Bernhardsson, David Waxman, Mattias Jakobsson, and Per Sjödin

Abstract

Ancient DNA (aDNA) can prove a valuable resource when investigating the evolutionary relationships between ancient and modern populations. Performing demographic inference using datasets that include aDNA samples however, requires statistical methods that explicitly account for the differences in drift expected among a temporally distributed sample. Such drift due to temporal structure can be challenging to discriminate from admixture from an unsampled, or "ghost", population, which can give rise to very similar summary statistics and confound methods commonly used in population genetics. Sequence data from ancient individuals also have unique characteristics, including short fragments, increased sequencing-error rates, and often limited genome-coverage that poses further challenges. Here we present a novel and conceptually simple approach for assessing questions of population continuity among a temporally distributed sample. We note that conditional on heterozygote sites in an individual genome at a particular point in time, the mean proportion of derived variants at those sites in other individuals has different expectations forwards in time and backwards in time. The difference in these processes enables us to construct a statistic that can detect population continuity in a temporal sample of genomes. We can show that the statistic is sensitive to historical admixture events from unsampled populations. Simulations are used to evaluate the power of this approach. We investigate a set of ancient genomes from Early Neolithic Scandinavia to assess levels of population continuity to an earlier Mesolithic individual. Individuals from hunter-gathering Neolithic Pitted Ware culture show marked continuity with the Mesolithic individual, whereas the contemporary Neolithic individuals from the and farming Funnel Beaker culture display much less continuity.

Introduction

Advances in DNA sequencing have led to rapidly increasing numbers of ancient genomes available for demographic inference. Understanding the relationships among such temporally distributed genomes is not only of fundamental interest (Sjödin, Skoglund, and Jakobsson, 2014; Malmström et al., 2009; Lazaridis et al., 2014; Slatkin, 2016; Schraiber, 2017), but can also help reveal historical demographic patterns that would be impossible to detect using modern genomes alone (Green et al., 2010; Lazaridis et al., 2016; Raghavan et al., 2014; Haak et al., 2015; Rasmussen et al., 2015). In the field of human evolution in particular, ancient genomes have been key to discriminating between models of population continuity, admixture and replacement that have accompanied the emergence and spread of technological innovations, cultures and languages around the world (Lazaridis et al., 2016; Skoglund et al., 2012; Raghavan et al., 2014; Haak et al., 2015; Rasmussen et al., 2015; Olalde et al., 2018).

The primary challenge when investigating population continuity among ancient genomes is that changes in population allele frequencies over time (due to

genetic drift) can lead to patterns of genetic differentiation among a temporally distributed sample that obscure continuity. Similar patterns can arise under models of historical admixture, particularly when the source of that admixture is an unsampled, "ghost" population (Beerli, 2004; Slatkin, 2005; Lawson, Dorp, and Falush, 2018). The confounding effects of such structure have been demonstrated using both model-based methods of inference (Städler et al., 2009; Rosen et al., 2018; Mazet et al., 2016) and more qualitative approaches (Lawson, Dorp, and Falush, 2018; McVean, 2009; François et al., 2019). Repeated findings of such unsampled admixture events in the histories of human populations (Green et al., 2010; Reich et al., 2010; Wall et al., 2019; Durvasula and Sankararaman, 2020) has spurred the development of methods that aim to detect and quantify ghost admixture in the ancestries of modern populations (Skov et al., 2018; Wall et al., 2019; Durvasula and Sankararaman, 2020).

A further challenge can be that due to the high levels of DNA fragmentation and contamination present (Allentoft et al., 2012; Skoglund et al., 2014b), ancient genomes are frequently sequenced to low coverage, without the depth necessary to confidently assign diploid genotypes (Dabney and Meyer, 2019). In the absence of the information that resides in patterns of linkage among loci, we are often limited to those inference methods based on genetic distances (Wang, Zollner, and Rosenberg, 2012; Verdu et al., 2014), diversity indices (Skoglund et al., 2014a; Diego-Ortega-Del and Montgomery, 2018), or allele frequency-based summary statistics (Patterson et al., 2012). Although the increasing availability of aDNA sequences has led to some temporally aware population genetic methods that explicitly account for the differences in drift expected among temporally distributed sequences (Sjödin, Skoglund, and Jakobsson, 2014; Yang and Montgomery, 2015; Rasmussen et al., 2015; Racimo, Renaud, and Slatkin, 2016; Schraiber, 2017; Silva et al., 2018; François and Jay, 2020), very often such techniques rely on good diploid calls, and therefore fail to take advantage of the large number of low coverage (<1X) ancient genomes available. Many commonly used methods do not explicitly account for the genetic drift expected among a temporally distributed sample, leading to contradictory or misleading results (Schraiber, 2017). The popular model-based clustering methods STRUCTURE and ADMIXTURE for instance, do not presently account for different temporal sampling schemes, which can result in distorted patterns of shared ancestry when a sample includes ancient genomes (François et al., 2019). The placement of individuals on Principle Components Analysis (PCA) projections has also been shown to reflect both the temporal and geographic distribution of samples (Skoglund et al., 2014a; Novembre and Stephens, 2008). Figure 1 demonstrates the confounding effect of such temporal structure. Datasets of temporally distributed samples were simulated under alternative demographic models of population continuity and historical admixture from an unsampled population, resulting in similar projections. High levels of branch-specific drift separating an ancient from modern populations can make it difficult to identify genuine cases of population continuity (Slatkin, 2016).

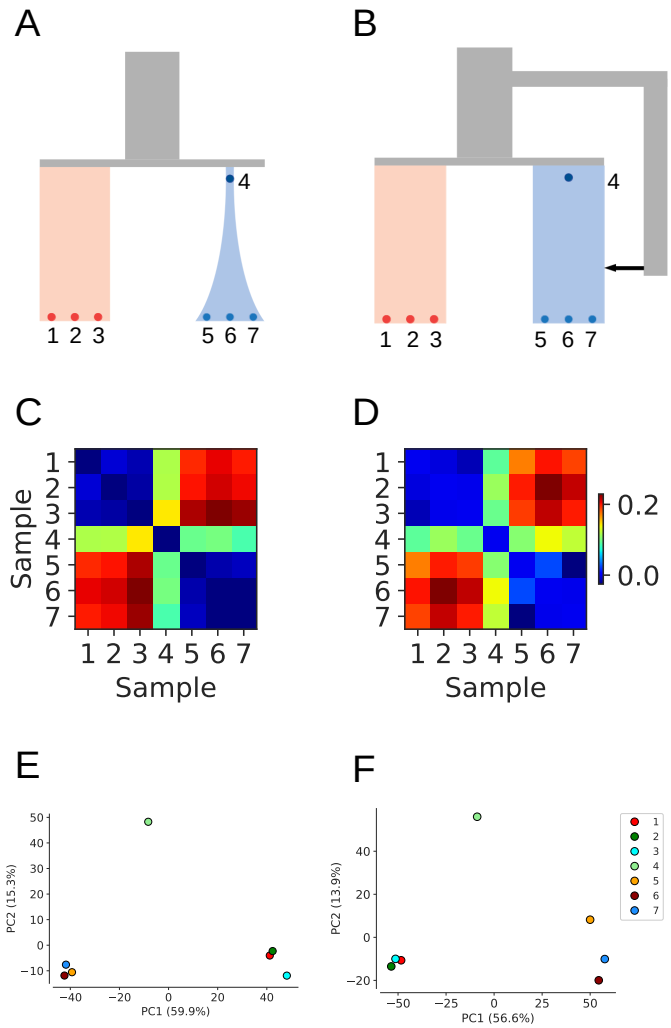

Figure 1: The confounding effects of temporal structure on demographic inference. Datasets simulated under alternative demographic models of A) population branch specific drift, and B) admixture from an unsampled population can result in highly similar pairwise f_2 matrices (C & D) and PCA projections (E & F). In both cases, high levels of drift between ancient and modern samples can obscure relationships of genuine population continuity. Simulations performed using msprime (Kelleher, Etheridge, and McVean, 2016), calculation of f_2-statistics and PCAs performed using scikit-allel (Miles, A. and Murillo, R. and Ralph, P. and Harding, N and Pisupati, R. and Rae, S. and Millar, T., 2010).

Various forms of 2, 3 and 4 populations or individuals tests, *f*-statistics, represents a powerful framework widely applied in population genetics studies (e.g., Green et al., 2010; Reich et al., 2010; Patterson et al., 2012; Haak et al., 2015; Olalde et al., 2018). Built upon the the expected covariance in allele frequency differences between populations, f_2, f_3 and f_4-statistics have been used to provide evidence for admixture events in the deep ancestry of modern humans (Green et al., 2010; Reich et al., 2010; Patterson et al., 2012). However the application of *f*-statistics is not limited to tests of admixture. Since they are capable of partitioning the total genetic drift separating samples into shared and private components of drift, they find general utility as statistical tests of tree-like relationships among populations. Using an unadmixed outgroup and assuming a simple divergence model relating two test populations, the f_3-statistic can be used to measure the shared drift between two test populations and the outgroup. (Peter, 2016) has shown that this test can be expressed as a sum of f_2-statistics:

$$f_3(O;X,Y) = \frac{1}{2}(f_2(O,X) + f_2(O,Y) - f_2(X,Y)) \tag{1}$$

The f_3-statistic could be re-formulated as a simple test of population continuity among a temporally distributed sample. Consider the case of a true outgroup and two individuals sampled at different times from the same population (figure 2). Under this set-up, samples X & Y will share an amount of drift equivalent to the branch length from the outgroup to the oldest sampled individual X. This holds because *f*-statistics are additive (unlike the closely related pairwise F_{ST}), meaning this result is not affected by the sampling time of the more recent individual (Y) or changes in population size along the branches of the tree (Patterson et al., 2012).

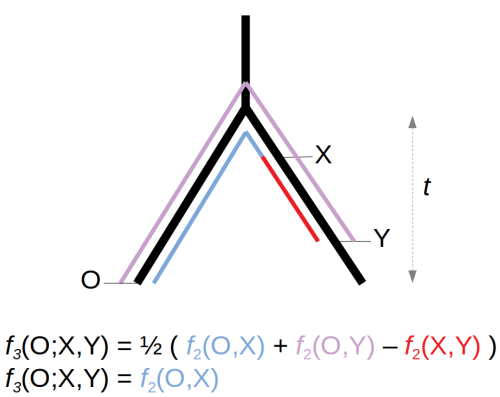

Figure 2: Application of f_3-statistic as a test for population continuity. With outgroup O and ancient individuals X and more recent Y sampled from the same population, the resulting f_3-statistic will be the same regardless of sampling time of Y.

Limitations exist for such a test of continuity however. Estimation of *f*-statistics usually requires correction to account for the upward bias in estimated genetic distances that can result from the inaccurate population allele frequency counts and missing data characteristic of small sample sizes and low coverages (Patterson et al., 2012). Perhaps the main caveat is that although the f_2-statistic measures the decay in heterozygosity between two individuals sampled at different time points from the same population (Peter, 2016), covariances in allele frequency differences do not constitute the most natural framework for quantifying levels of drift among temporally structured samples.

Here we propose a novel and conceptually simpler approach for detecting population continuity among a temporally distributed sample. The approach is sensitive to historical admixture from unsampled populations. It can further be used with modest coverage ancient genomes and it is robust to missing data. The principle underlying the approach is simple; conditioning on a large number of heterozygote sites in an individual sampled from a population at a particular point in time, the mean proportion of derived alleles at those sites in other individuals is affected differently by the action of genetic drift forwards and backwards in time. The different expectations for these processes allows us to differentiate between models of population continuity and admixture, and in certain cases, to estimate the proportion of ghost admixture that has occurred. We evaluate the utility and power of this approach using simulations and apply the method to a set of ancient genomes sequenced from a Scandinavian Mesolithic forager, five hunter-gatherers from the Neolithic Pitted Ware Culture (PWC) and four contemporaneous farmers from the Funnelbeaker Culture (TRB).

Method

We will first outline the theory behind the model, followed by the derivation of the central summary-statistic and finally describe a set of simulations that illustrate the the approach.

Theory

Although allele frequencies change over time, it is a well established fact of population genetics that given a population frequency of p of a neutral variant, the expected population frequency of this variant will remain indefinitely at p forward in time (Kimura and Ohta, 1969). Consequently, since all (neutral) variants are eventually either lost or fixed in the population, the fixation probability of an allele at present population frequency p is p. This holds regardless of whether the frequency of the derived or the ancestral variant is considered. On the contrary, the expected frequency of a derived variant looking backwards in time cannot be the same as the present frequency simply because we know that it will eventually disappear (at the time of the mutation that gave rise to it). In fact, we show in the appendix that the expected frequency of a derived variant t

generations ago given a present frequency p is $pe^{-\tau}$ where τ is the scaled time or drift between now and t generations ago ($\tau = t/2Ne$). To illustrate, in figure 3, conditional on population frequency p in population A, the expected frequency of the derived variant in the branch below population A is p (independent of τ_1) while the expected frequency of the derived variant in the right population branch is $pe^{-\tau_2}$ (independent of τ_3).

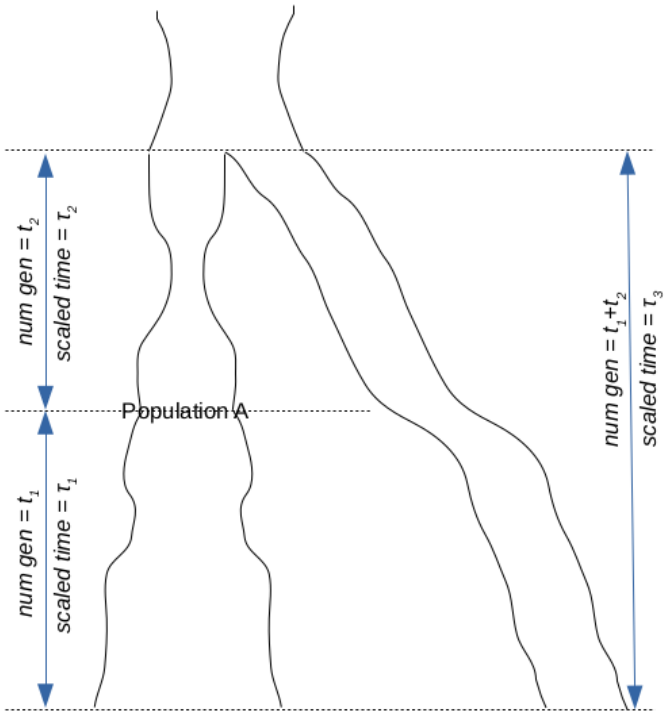

Figure 3: An illustration of the model being analyzed when the two most recent populations are at the same generation. Note however that since scaled time is different from the number of generations, τ_3 may be different from $\tau_1 + \tau_2$.

Now consider that an individual (the "anchor" individual for brevity) has been sequenced and genotypes have been called. If we restrict the analysis to heterozygote sites (and we assume that the ancestral and derived variant is known), we know that the derived variant is at least as old as the anchor individual. We also that it is neither fixed nor lost at this time point which allows us to use the diffusion theory results of the Appendix. The population frequency of the derived variant is not the same at all of these heterozygote sites, but the conditioned distribution has an expected value which we will denote by

$\overline{p_A}$ where

$$\overline{p_A} = E[X_A|\text{one derived and one ancestral variant in population A}]$$
$$= \int_0^1 x f(\text{population frequency } X_A = x|\text{one derived and one ancestral variant in population A})dx$$

Thus, if we refer to this set of heterozygote sites in the anchor individual as H_A, the probability to draw the derived variant at a site in the set H_A — in the same population that the anchor individual was sampled from — is $\overline{p_A}$. Moreover, for any individual that lived more recent in time and that traces all of its ancestry to population A, the probability to draw the derived variant among H_A is also $\overline{p_A}$. Such an individual can be said to be sampled from a population that is completely continuous with the population the anchor individual was sampled from. It can also be useful to quantify some lower level of continuity as a fraction of complete continuity. There are several ways of doing this, but we will mainly rely on the average –*backwards in time* – genetic drift when following the path *from* an anchor population *to* the test population. We refer to this measure as the β-drift of a test population/individual relative to an anchor population/individual. Here, β-drift = 0 implies complete continuity. See appendix for a fuller discussion of continuity and β-drift.

The anchor statistic

Given an anchor individual A and a set H_A of heterozygous sites in A, we define the *anchor statistic* (sometimes simply the *proportion derived* variants) for a test individual x as the probability to draw the derived variant in x at sites in H_A. In practice, for low coverage data we do this by adding $k/(k+l)$, where k is the number of reads supporting the derived and k is the number of reads supporting the ancestral, for all sites with $k+l > 0$ and then dividing by the total number of sites (among the H_A sites) with $k+l > 0$. For high coverage data we would just use the number of heterozygous sites (n_{het}), the number of homozygous derived sites (n_{der}) and the number of homozygous ancestral sites (n_{anc}) among the H_A anchor sites and do $(0.5n_{het} + n_{der})/(n_{het} + n_{der} + n_{anc})$. Incidentally, this is conceptually similar to how pseudo-haploidization sometimes is performed.

Estimating admixture

Consider an individual that traces an amount $1 - \gamma$ of its genetic ancestry to the anchor population but a proportion γ of its genetics ancestry comes from a population that diverged from the anchor population branch τ units of genetic drift prior to the anchor population. The average frequency at the time of the split of the latter population (and hence in all of that branch forwards in time) is then $\overline{p_A}e^{-\tau}$ (see above). The probability to draw the derived variant among H_A is therefore no longer $\overline{p_A}$ but

$$(1-\gamma)\overline{p_A} + \gamma\overline{p_A}e^{-\tau} = \overline{p_A}(1 - \gamma(1 - e^{-\tau}))$$

Next, consider the model set-up shown in figure 4(a). If we sample four genomes, (A_1, A_2, B and C), of which A_1 is assumed older than, but continuous with A_2 and B. C is assumed to be sampled more recently than the others and the admixture event. The admixture event comprises a proportion γ from a population diverging τ time units back from A_1, and $\tau + \tau_A$ drift units back from sample A_2.

If by $E_i[X_j]$ we denote the expected proportion of derived variants (the anchor statistic) in a sample from population j among sites that are heterozygote in the anchor sample from population i, then

$$\begin{aligned}
E_{A_1}[X_B] &= E_{A_1}[X_{A_2}] = \overline{p_{A_1}} \\
E_{A_1}[X_C] &= \overline{p_{A_1}}\left(1 - \gamma(1 - e^{-\tau})\right) \\
E_{A_2}[X_B] &= \overline{p_{A_2}} \\
E_{A_2}[X_{A_1}] &= \overline{p_{A_2}} e^{-\tau_A} \\
E_{A_2}[X_C] &= \overline{p_{A_2}}\left(1 - \gamma(1 - e^{-(\tau+\tau_A)})\right)
\end{aligned}$$

Furthermore, if we allow private drift to each of the sampled individuals so that, in effect, there is no contribution from any of the possible anchor populations to any of the possible test individuals, (see figure 4(b)) as well as sequencing errors private to the anchors (denoted by ϵ_{A_1} and ϵ_{A_2}) we have

$$\begin{aligned}
E_{A_1}[X_B] &= E_{A_1}[X_{A_2}] = (1 - \epsilon_{A_1}) e^{-\tau_{A_1}} \overline{p_{A_1}} \\
E_{A_1}[X_C] &= (1 - \epsilon_{A_1}) e^{-\tau_{A_1}} \overline{p_{A_1}}\left(1 - \gamma(1 - e^{-\tau})\right) \\
E_{A_2}[X_B] &= (1 - \epsilon_{A_2}) e^{-\tau_{A_2}} \overline{p_{A_2}} \\
E_{A_2}[X_{A_1}] &= (1 - \epsilon_{A_2}) e^{-\tau_{A_2}} \overline{p_{A_2}} e^{-\tau_A} \\
E_{A_2}[X_C] &= (1 - \epsilon_{A_2}) e^{-\tau_{A_2}} \overline{p_{A_2}}\left(1 - \gamma(1 - e^{-(\tau+\tau_A)})\right)
\end{aligned}$$

In effect, this is the same as a rescaling of $\overline{p_{A_2}}$ and $\overline{p_{A_2}}$ and for both figure 4(a) and figure 4(b) we have

$$\gamma = 1 - \frac{E_{A_1}[X_B]E_{A_2}[X_C] - E_{A_1}[X_C]E_{A_2}[X_{A_1}]}{E_{A_1}[X_B]E_{A_2}[X_B] - E_{A_1}[X_B]E_{A_2}[X_{A_1}]} \tag{2}$$

where γ is the proportion of ancestry in C from the "ghost" population to the right.

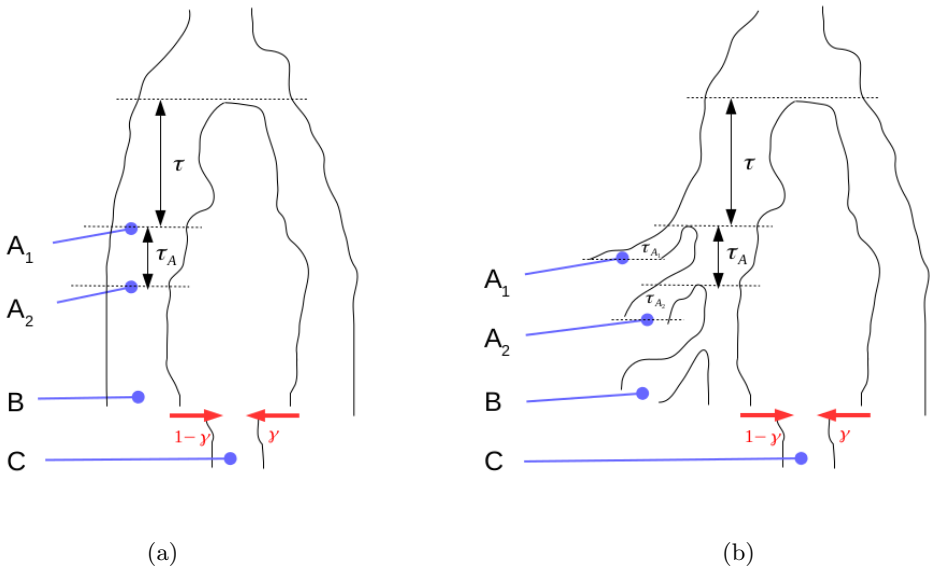

Figure 4: Set up for estimating proportion of admixture (γ) from a population diverging τ time units before anchor sample A_1.

Simulations

Detecting population continuity and quantifying admixture

Here we use simulations to investigate the power of this approach to detect population continuity and quantify admixture from an unsampled population. Datasets were simulated under alternative demographic models of population continuity (figure 5A), and population discontinuity including two pulses of admixture from a population diverging 4000 generations ago (figure 5B). All simulations were performed using msprime (Kelleher, Etheridge, and McVean, 2016), aggregating data across 1000 runs of a 2M base sequence.

In each model, 7 diploid individuals were sampled at times ranging from present day to 720 generations in the past. The generation time was set to 29 years, with mutation and recombination rates fixed at 1.45×10^{-8} and 1.25×10^{-8} respectively. Both models include a population divergence event 4000 generations in the past, with a population experiencing an expansion from $N = 1000$ at divergence time to $N = 10000$ at present day. All other branches of the models are fixed and constant at N=10000 to aid evaluation of model accuracy. Note however, that the anchor framework requires no assumption of fixed or constant population sizes through time to detect population continuity or ghost admixture. Model B in Figure 5 includes two pulses of 25% admixture from the diverging population at 180 and 420 generations respectively. We can condition on heterozygote sites in the oldest individual from our sample (individual 1 sampled at 720 generations) in both models, and compare the mean proportion

of derived at those sites in more recent individuals.

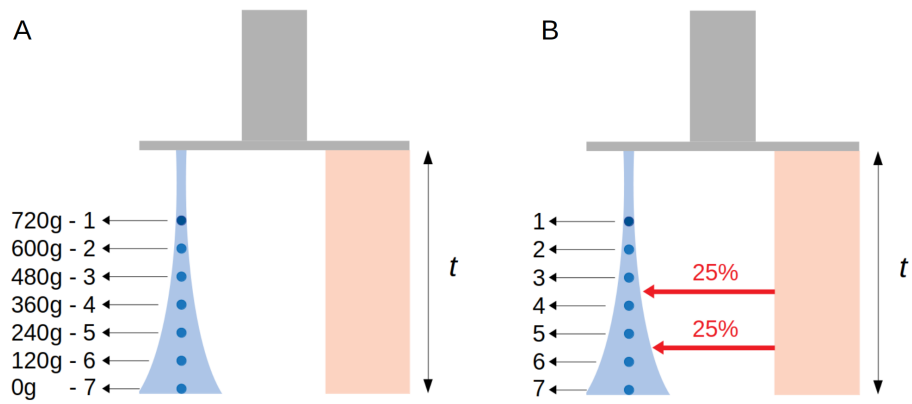

Figure 5: Illustrating the set-up used for simulation of data under models of A) population continuity and B) pulsed admixture from an unsampled population. Samples $1-7$ are taken at different time points from one population undergoing a population expansion from initial size at population divergence of $1,000$ diploid individuals, to final size at present day of $10,000$. Times shown in generations with 1 gen=29 years. Population divergence time $t = 4,000$ generations.

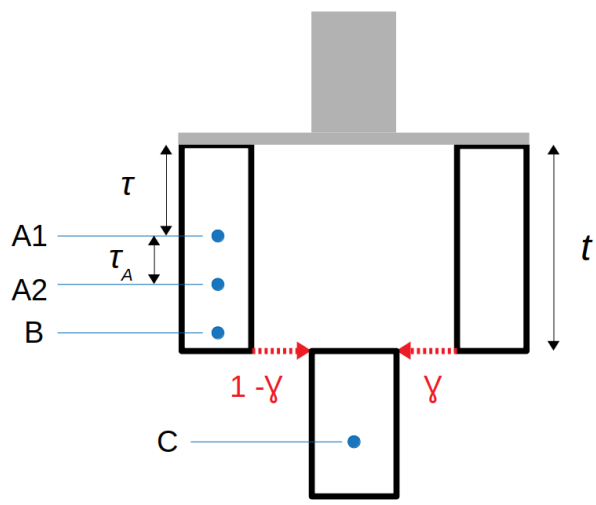

Figure 6: Simulation model set up for estimating proportion of admixture (γ) from a population diverging τ time units before anchor sample A_1.

In order to evaluate the power of this framework to estimate admixture proportions from an unsampled population, a dataset was simulated under the

demographic model of a pulse admixture event shown in figure 6. Simulations were performed in an identical manner as before, but this time with four individuals (A_1, A_2, B and C) sampled at $1,000$, 100, 50 and 0 generations respectively. A single pulse of admixture into this temporal sample was included at 25 generations in the past (between sampling times of individuals B and C). The performance of the anchor test in estimating admixture proportions was assessed when three parameters of this model were allowed to vary; admixture proportions (γ) varying from 0% to 90%, population divergence time t ranging from $1,000$ to $5,500$ generations, and the degree of drift in the branch separating anchor samples (time separating individuals A_1 and A_2 allowed to vary between 100 and 900 generations).

Results

Simulations

Detecting population continuity and ghost admixture

Figure 7 shows the mean proportion derived variants in individuals more recent than the anchor-individual, for simulated data from models of population continuity and admixture. Forward in time, the mean proportion derived variants remains constant under a model of population continuity even in the presence of strong branch specific genetic drift followed by population expansion (figure 5A). Under a model of historical admixture however (figure 5B), there are two clear successive reductions in the mean proportion derived, each associated with separate admixture events. The magnitude of the reduction in proportion derived is a function of the degree of drift along the branch between the anchor-individual (individual 1) and the population divergence event ($t = 4,000$) giving rise to the population that mixes into the sampled population, together with the proportion of admixture (0.25 in each pulse).

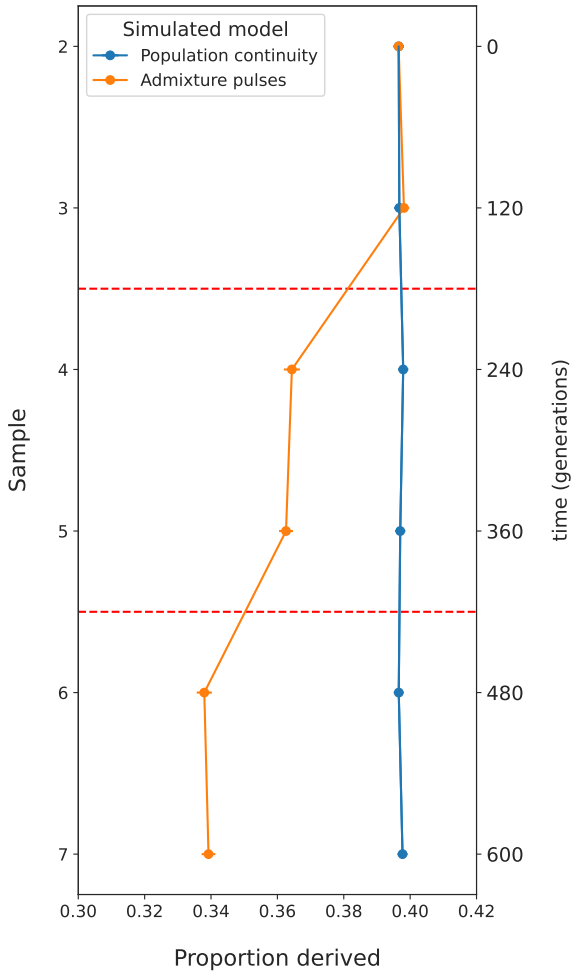

Figure 7: Anchor statistic under simulated models of population continuity and admixture. In each case the oldest sampled individual (1) is used as the anchor-individual, with the mean proportion derived at anchor heterozygote sites counted in all more recent individuals. Red dashed lines at $t = 180$ & $t = 420$ generations indicate admixture events (25%) in the Admixture Pulse model. The mean proportion derived variants remains constant forwards in time for individuals sampled from a model of population continuity. The mean proportion derived variants shows successive reductions for individuals sampled from a model that includes admixture. Error bars show two weighted-block jackknife standard errors.

Estimating admixture proportions

The mean proportion derived variants can also be used to estimate admixture as outlined in the Methods section. From simulations, we show that this framework in predicting the admixture proportion is highly correlated to the true admixture proportion ($r = 0.98$, Pearson correlation). Furthermore, the accuracy of the admixture-estimate does not appear to be affected by the true proportion of admixture itself (figure 8a). Varying the population divergence time (t) from 1000 to 5500 generations does not change to accuracy of the estimation (figure 8b). Figure 8c shows that admixture estimation uncertainty increases as the degree of drift between anchor-individuals is reduced from 900 to 100 generations. These observations suggest that it is not the genetic drift prior to the anchor-individuals, but rather the degree of drift between the two anchor samples that influence accuracy of admixture estimation.

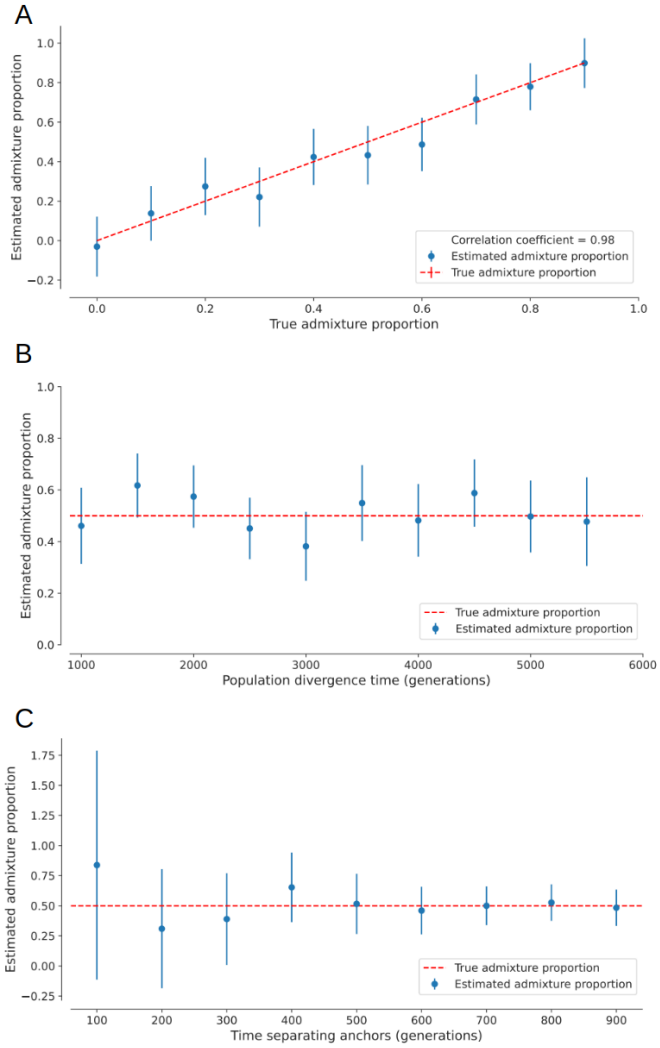

Figure 8: Estimating admixture proportions from an unsampled population with A) a fixed divergence time (t) of 4000 generations and admixture proportions varying from 0 to 0.9, B) a fixed admixture proportion of 0.5 and t varying from 1000 to 5500 generations, and C) a fixed admixture proportion of 0.5 and t of 4000 generations, with time separating anchors A_1 and A_2 ranging from 100 to 900 generations. In each case, sampling time of anchor-individual A_1 is 1000 generations and population sizes are constant at $10,000$ diploid individuals. Error bars show two weighted-block jackknife standard errors.

Estimating admixture proportion among a temporal sample therefore requires two individuals of sufficiently high coverage that heterozygotes can be

confidently called, and for those anchor individuals to be sampled far enough apart to gain the necessary power for accurate estimation.

Investigating population continuity from Mesolithic foragers to different Neolithic groups in Scandinavia

Scandinavia as a region holds special interest when considering the roles that population continuity and admixture have had on the emergence and spread of human cultures. It was the last region of Europe to become free of ice after the Last Glacial Maximum (LGM), and it harboured some of the last populations of hunter-gatherers in Europe. The earliest expressions of Neolithic material culture also emerged relatively late, with the arrival of the Funnelbeaker culture (TRB) circa 3500BCE to southern Scandinavia (Midgley, 1992; Lillie et al., 2000; Skoglund et al., 2012; Fraser et al., 2018). Paleogenetic data show a close connection between these early farmers of Scandinavia and other Early and Middle Neolithic farmers of Europe (Malmström et al., 2015; Malmström et al., 2019), providing strong support for a model of population discontinuity between the Scandinavian hunter-gatherers of the Mesolithic and the arriving farmers. The Neolithic Pitted Ware Culture (PWC) represents an intriguing case of a hunter-gathering culture in Scandinavia that emerge circa 3200BCE and post-dates the migration of the farmers that spread the TRB culture into Scandinavia. Despite this, the results of several studies have indicated that the PWC culture predominantly shows genetic affinity to earlier Mesolithic hunter-gatherers rather than contemporary Neolithic farmers (Skoglund et al., 2012; Skoglund et al., 2014a). Furthermore, archaeological data has been used to paint a picture of two cultures overlapping in both time and space, coexisting in parallel for several hundred years and yet still maintaining distinct material cultures and dietary patterns, in addition to maintaining distinct genetic make-ups (Malmström et al., 2009; Fraser et al., 2018; Coutinho et al., 2020; Malmström et al., 2019).

We assembled a panel of high-coverage ancient genomes from an ongoing effort to increase genome coverage from Scandinavian Stone Age humans, including a Mesolithic hunter-gatherer from the Baltic Island Stora Karlsö (sf12) and five PWC hunter-gatherers from the Baltic island of Gotland, together with four TRB farmers from the Megalithic passage tombs of Gökhem and Rössberga (supplementary table 1, Günther et al., 2018; Fraser et al., 2018; Coutinho et al., 2020; Malmström et al., 2019). Although from distinct material cultures, all PWC and TRB individuals are broadly contemporaneous from the same period of the Nordic Middle Neolithic (circa $3200 - 2300$BCE). The raw sequence data was processed according to Alves *et al* (2022) (Alves et al., 2022) and Günther *et al* (2018) (Günther et al., 2018), and per sample diploid VCF files were created with snpAD (Prüfer, 2018).

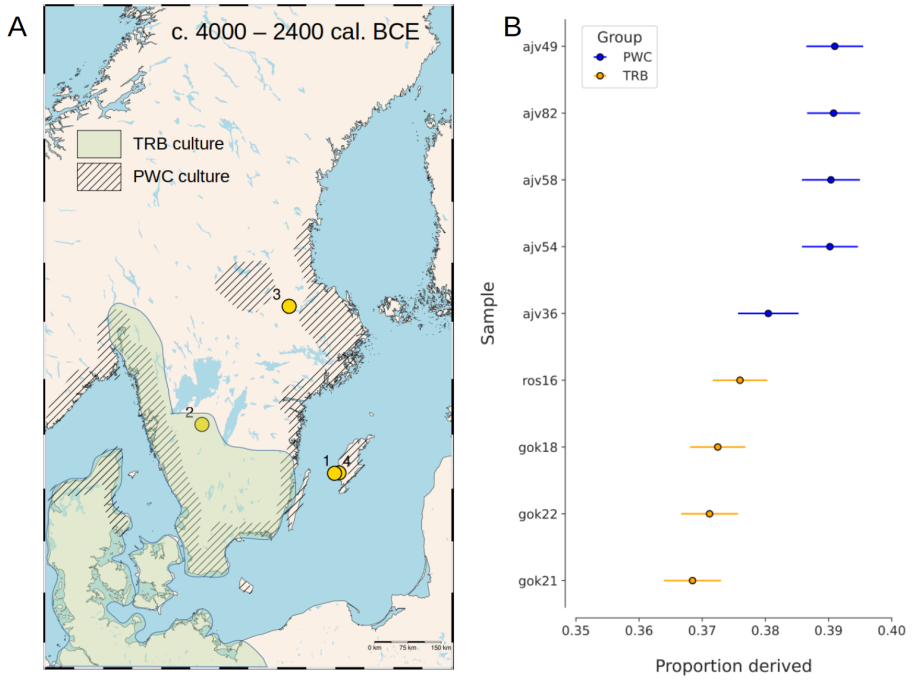

Figure 9: A) Map showing distributions of the Funnel Beaker culture (TRB), and the sub-Neolithic Pitted Ware culture (PWC) during the Nordic Middle Neolithic period. All PWC individuals from 1. Ajvide burial, Gotland. TRB burial sites sampled include 2. Gökhem passage grave, and 3. Rössberga passage grave. Mesolithic individual sf12 from 4) Stora Förvar on Stora Karlsö. The map was adapted from (Malmström et al., 2009) and plotted using python package (Uieda et al., 2022). B) Results of anchor test of population continuity, with Scandinavian Mesolithic hunter-gatherer sf12 used as anchor. Although ajv36 encountered more β-drift from sf12 than the other PWC individuals, the results are consistent with the PWC hunter-gatherers being continuous with sf12 while the TRB farmers show clear discontinuity with both sf12 and the PWC individuals. Error bars show two weighted-block jackknife standard errors.

The Mesolithic hunter-gatherer sf12 was used as the anchor-individual so as to measure continuity between this individual and a set of other, more recent, individuals. The mean proportion derived variants (conditional on being variable in the anchor-individual sf12) in more recent individuals from the PWC and TRB cultures are shown in figure 9B. All PWC individuals (except ajv36) show a higher and similar mean proportion derived variants. Thus, there appears to be lower and equal amounts of β-drift among the PWC individuals compared to the TRB individuals. This is consistent with population continuity from the PWC individuals to the population sf12 belonged to. All TRB farmer individuals show significantly lower mean proportion derived, implying a larger amount

of β-drift suggesting clear population discontinuity with the Mesolithic individual as well as with the PWC individuals. These results are consistent with previous findings of modest gene-flow between the contemporaneous PWC and TRB groups (Malmström et al., 2009; Fraser et al., 2018; Coutinho et al., 2020). Interestingly however, the PWC individual ajv36 shows a significant increase in β-drift relative to the other PWC individuals. This observation can be due to admixture with the people of the TRB culture. To investigate this finding further, a four-population test of admixture (also known as the "ABBA-BABA test" (Patterson et al., 2012)) was performed of form D(Ballito bay Boy, test-individual ; sf12, LBK) using the ancient African individual Ballito Bay Boy as an outgroup (Schlebusch et al., 2017), and testing for excess sharing of alleles between each of our sampled individuals and the Mesolithic hunter gatherer sf12 and an Early Neolithic farming individual from central Europe (which is known as the 'LBK'-individual). This test provides evidence that the ajv36 individual shares increased drift with Neolithic farmers relative to all other PWC individuals in this study (supplementary figure 11), consistent with gene-flow from a group related to Neolithic farmers. While some studies have found low levels of admixture between contemporaneous TRB and PWC groups, (Skoglund et al., 2014a; Günther et al., 2018; Mittnik et al., 2018), it is intriguing to note that ajv36 has greater level than other individuals from the same burial site and culture, suggesting that there was some level of ongoing gene-flow from the farmers into the PWC hunter-gatherers.

Given that investigating population discontinuity using the anchor framework fundamentally depends on a reduction in the mean proportion derived at a set of sites ascertained in another "anchor"-individual, there is a risk of false positives arising either from stochastic subsampling of sites in very low coverage samples, or from sequencing errors that tend to be slightly greater in genomes sequenced from the remains of post-mortem individuals. To evaluate the robustness of this approach against biases stemming from low coverages, we downsampled a PWC individual from a mean autosomal coverage of $\sim$ 17X to $\sim$ 1X and repeated our analyses. Supplementary figure 12 shows an increase in the size of confidence intervals for the downsampled individual, but no significant change in overall results. Hence, the point estimate of the anchor-statistic appears to be largely unaffected, but the confidence of the point-estimate decrease.

Discussion

Ancient genomes have the capacity to revolutionize our understanding of the demographic processes contributing to patterns of genetic variation among current-day humans as well as among other species. aDNA can reveal population continuity through time and aid in the detection of historical admixture events and population replacements. Particularly in studies of human demographic history, aDNA has proven an important resource in understanding the pre-historic movements of people that have spread cultures, languages, and technologies to

new areas. In order to take full advantage of this resource however, it is essential to develop population genetic tools capable of utilizing samples of temporally distributed genomic data.

Here we have outlined a novel and conceptually simple approach capable of detecting population continuity through time. It is sensitive to admixture from unsampled ("ghost") populations and can take advantage of the increasing numbers of low coverage genomes available. We have shown, through simulations and an empirical example, that this approach has the power to infer population continuity and estimate proportions of ghost admixture.

Acknowledgement

We want to thank Olaf Thalmann, Karl-Heinz Herzig, and Jarosoław Walkowiak for access to unpublished data, Nikola Vukovic for help with graphic design and Imke Lankheet for Latex assistance. This work was supported by the Knut and Alice Wallenberg foundation. The computations and data handling were enabled by resources (SNIC2022/2-11 and p2018003) provided by the Swedish National Infrastructure for Computing (SNIC) at UPPMAX.

References

Allentoft, Morten E et al. (2012). "The half-life of DNA in bone: measuring decay kinetics in 158 dated fossils". In: *Proceedings of the Royal Society B: Biological Sciences* 279.1748, pp. 4724–4733.

Alves, Isabel et al. (2022). "Genetic population structure across Brittany and the downstream Loire basin provides new insights on the demographic history of Western Europe". In: *bioRxiv*. DOI: 10.1101/2022.02.03.478491. eprint: https://www.biorxiv.org/content/early/2022/02/04/2022.02.03.478491.full.pdf. URL: https://www.biorxiv.org/content/early/2022/02/04/2022.02.03.478491.

Beerli, P. (2004). "Effect of unsampled populations on the estimation of population sizes and migration rates between sampled populations". In: *Mol Ecol* 13, pp. 827–836.

Blank, M., KG. Sjögren, and J. Storå (2020). "Old bones or early graves? Megalithic burial sequences in southern Sweden based on 14C datings". In: *Archaeological and Anthropological Sciences* 12 (89), pp. 1866–9565. DOI: 10.1007/s12520-020-01039-9.

Coutinho, Alexandra et al. (2020). "The Neolithic Pitted Ware culture foragers were culturally but not genetically influenced by the Battle Axe culture herders". In: *American Journal of Physical Anthropology* 172.4, pp. 638–649. DOI: https://doi.org/10.1002/ajpa.24079. eprint: https://onlinelibrary.wiley.com/doi/pdf/10.1002/ajpa.24079. URL: https://onlinelibrary.wiley.com/doi/abs/10.1002/ajpa.24079.

Dabney, Jesse and Matthias Meyer (2019). "Extraction of highly degraded DNA from ancient bones and teeth". In: *Ancient DNA*. Springer, pp. 25–29.

Diego-Ortega-Del, V. and S. Montgomery (2018). "FST between Archaic and Present-Day Samples". In: *bioRxiv*. DOI: 10.1101/362053.

Durvasula, A. and S. Sankararaman (2020). "Recovering signals of ghost archaic introgression in African populations". In: *Science Advances* 6.7. DOI: 10.1126/sciadv.aax5097.

François, O. et al. (2019). "Inference of population genetic structure from temporal samples of DNA". In: *bioRxiv*. DOI: 10.1101/801324.

François, Olivier and Flora Jay (2020). "Factor analysis of ancient population genomic samples". In: *Nature communications* 11.1, pp. 1–11.

Fraser, Magdalena et al. (2018). "New insights on cultural dualism and population structure in the Middle Neolithic Funnel Beaker culture on the island of Gotland". In: *Journal of Archaeological Science: Reports* 17, pp. 325–334.

Green, RE. et al. (2010). "A Draft Sequence of the Neandertal Genome". In: *Science* 328.5979, pp. 710–722. DOI: 10.1126/science.1188021.

Griffiths, RC (2003). "The frequency spectrum of a mutation, and its age, in a general diffusion model". In: *Theor. Popul. Biol.* 64, pp. 241–251.

Günther, T. et al. (Jan. 2018). "Population genomics of Mesolithic Scandinavia: Investigating early postglacial migration routes and high-latitude adaptation". In: *PLOS Biology* 16.1, pp. 1–22. DOI: 10.1371/journal.pbio.2003703. URL: https://doi.org/10.1371/journal.pbio.2003703.

Haak, W. et al. (Mar. 2015). "Massive migration from the steppe was a source for Indo-European languages in Europe". In: *Nature* 522.7555, p. 207. DOI: 10.1038/nature14317.

Kelleher, J., AM. Etheridge, and G. McVean (2016). "Efficient Coalescent Simulation and Genealogical Analysis for Large Sample Sizes". In: *PLoS Comput Biol* 12, e1004842. DOI: 10.1371/journal.pcbi.1004842.

Kimura, M. and T. Ohta (1969). "The average number of generations until fixation of a mutant gene in a population". In: *Genetics* 61, pp. 763–771.

Lawson, DJ., L. van Dorp, and D. Falush (2018). "A tutorial on how not to over-interpret STRUCTURE and ADMIXTURE bar plots". In: *Nat Commun* 9.3258. DOI: 10.1038/s41467-018-05257-7.

Lazaridis, I. et al. (2014). "Ancient human genomes suggest three ancestral populations for present-day Europeans". In: *Nature*, pp. 409–13. DOI: 10.1038/nature13673.

Lazaridis, I. et al. (2016). "Genomic insights into the origin of farming in the ancient Near East". In: *Nature*, pp. 1476–4687. DOI: 10.1038/nature19310.

Lillie, Malcolm et al. (2000). *Europe's first farmers*. Cambridge University Press.

Malmström, Helena et al. (2015). "Ancient mitochondrial DNA from the northern fringe of the Neolithic farming expansion in Europe sheds light on the dispersion process". In: *Philosophical Transactions of the Royal Society B: Biological Sciences* 370.1660, p. 20130373.

Malmström, H. et al. (2009). "Ancient DNA Reveals Lack of Continuity between Neolithic Hunter-Gatherers and Contemporary Scandinavians". In: *Curr. Biol.* 19.20, pp. 1758–1762.

Malmström, H. et al. (2019). "The genomic ancestry of the Scandinavian Battle Axe Culture people and their relation to the broader Corded Ware horizon". In: *Proceedings of the Royal Society B* 286. DOI: 10.1098/rspb.2019.1528.

Mazet, O. et al. (2016). "On the importance of being structured: instantaneous coalescence rates and human evolution–lessons for ancestral population size inference?" In: *Heredity* 116, pp. 362–371. DOI: 10.1038/hdy.2015.104.

McVean, G. (2009). "A genealogical interpretation of principal components analysis". In: *Nature* 5.10, e1000686. DOI: 10.1371/journal.pgen.1000686.

Midgley, Magdalena (1992). "TRB culture. The first farmers of the north European plain." In.

Miles, A. and Murillo, R. and Ralph, P. and Harding, N and Pisupati, R. and Rae, S. and Millar, T. (Feb. 19, 2010). *scikit-allel*. Version 1.3.3. DOI: doi.org/10.5281/zenodo.4759368.

Mittnik, Alissa et al. (2018). "The genetic prehistory of the Baltic Sea region". In: *Nature communications* 9.1, pp. 1–11.

Novembre, J. and M. Stephens (2008). "Interpreting principal component analyses of spatial population genetic variation". In: *Nat Genet* 40, pp. 646–649.

Olalde, Iñigo et al. (2018). "The Beaker phenomenon and the genomic transformation of northwest Europe". In: *Nature* 555.7695, pp. 190–196.

Patterson, N. et al. (2012). "Ancient admixture in human history". In: *Genetics* 192, pp. 1065–1093. DOI: 10.1534/genetics.112.145037.

Paulsson, Bettina Schulz (2010). "Scandinavian models: Radiocarbon dates and the origin and spreading of passage graves in Sweden and Denmark". In: *Radiocarbon* 52.3, pp. 1002–1017.

Peter, BM. (2016). "Admixture, Population Structure, and F-Statistics". In: *Genetics* 202, pp. 1485–1501. DOI: 10.1534/genetics.115.183913.

Prüfer, Kay (2018). "snpAD: An ancient DNA genotype caller". In: *Bioinformatics* 34.24, pp. 4165–4171.

Racimo, F., G. Renaud, and M. Slatkin (2016). "Joint Estimation of Contamination, Error and Demography for Nuclear DNA from Ancient Humans". In: *PLOS Genetics* 12.4, pp. 1–27. DOI: 10.1371/journal.pgen.1005972.

Raghavan, M. et al. (2014). "The genetic prehistory of the New World Arctic". In: *Science* 345.6200, p. 1255832. DOI: 10.1126/science.1255832.

Rasmussen, M. et al. (2015). "The ancestry and affiliations of Kennewick Man". In: *Nature* 523, pp. 455–458. DOI: 10.1038/nature14625.

Reich, D. et al. (2010). "Genetic history of an archaic hominin group from Denisova Cave in Siberia". In: *Nature* 468, pp. 1053–1060. DOI: 10.1038/nature09710.

Rosen, Z. et al. (2018). "Geometry of the Sample Frequency Spectrum and the Perils of Demographic Inference". In: *Genetics* 210.2, pp. 665–682.

Schlebusch, CM. et al. (2017). "Southern African ancient genomes estimate modern human divergence to 350,000 to 260,000 years ago". In: *Science* 358.6363, pp. 652–655. DOI: 10.1126/science.aao6266.

Schraiber, JG. (2017). "Assessing the Relationship of Ancient and Modern Populations". In: *Genetics*. DOI: 10.1534/genetics.117.300448.

Silva, Nuno Miguel et al. (2018). "Bayesian estimation of partial population continuity using ancient DNA and spatially explicit simulations". In: *Evolutionary applications* 11.9, pp. 1642–1655.

Sjödin, P., P. Skoglund, and M. Jakobsson (2014). "Assessing the Maximum Contribution from Ancient Populations". In: *Molecular Biology and Evolution* 31.5, pp. 1248–1260. DOI: 10.1093/molbev/msu059.

Skoglund, P. et al. (2012). "Origins and genetic legacy of Neolithic farmers and hunter-gatherers in Europe". In: *Science* 336, pp. 466–469.

Skoglund, P. et al. (2014a). "Investigating population history using temporal genetic differentiation". In: *Mol Biol Evol* 31, pp. 2516–2527. DOI: 10.1093/molbev/msu192.

Skoglund, Pontus et al. (2014b). "Separating endogenous ancient DNA from modern day contamination in a Siberian Neandertal". In: *Proceedings of the National Academy of Sciences* 111.6, pp. 2229–2234.

Skov, Laurits et al. (Sept. 2018). "Detecting archaic introgression using an unadmixed outgroup". In: *PLOS Genetics* 14.9, pp. 1–15. DOI: 10.1371/journal.pgen.1007641. URL: https://doi.org/10.1371/journal.pgen.1007641.

Slatkin, M. (2005). "Seeing ghosts: the effect of unsampled populations on migration rates estimated for sampled populations". In: *Molecular ecology* 14, pp. 67–73.

— (2016). "Statistical methods for analyzing ancient DNA from hominins". In: *Curr Opin Genet Dev* 41, pp. 72–76.

Städler, T. et al. (2009). "The impact of sampling schemes on the site frequency spectrum in nonequilibrium subdivided populations". In: *Genetics* 182, pp. 961–965. DOI: 10.1534/genetics.108.094904.

Tavaré, S. (1984). "Line-of-Descent and Genealogical Processes, and Their Apllications in Population Genetics Models". In: *Theor. Popul. Biol.* 26, pp. 119–164.

Uieda, L. et al. (July 2022). *PyGMT: A Python interface for the Generic Mapping Tools*. Version v0.7.0. DOI: 10.5281/zenodo.6702566.

Verdu, P. et al. (2014). "Patterns of Admixture and Population Structure in Native Populations of Northwest North America". In: *PLOS Genetics* 10.8, pp. 1–17. DOI: 10.1371/journal.pgen.1004530.

Wakeley, J. (2009). *Coalescent Theory: An Introduction*. 1st. Greenswood Village, Colorado: Roberts & Company Publishers.

Wall, Jeffrey D et al. (2019). "Identification of African-specific admixture between modern and archaic humans". In: *The American Journal of Human Genetics* 105.6, pp. 1254–1261.

Wallin, P. and H. Martinsson-Wallin (2016). "Decoding Neolithic Atlantic and Mediterranean Island Ritual". In: Oxbow books. Chap. Collective spaces and material expressions: ritual practice and island identities in Neolithic Gotland.

Wang, C., S. Zollner, and NA. Rosenberg (2012). "A quantitative comparison of the similarity between genes and geography in worldwide human populations". In: *PLoS Genet* 8, e1002886.

Yang, MA. and S. Montgomery (2015). "Using Ancient Samples in Projection Analysis". In: *G3* 6, pp. 99–105.

Appendix

Moments for the population frequency

For brevity, we suppress the dependence of p and τ in the notation and write $E[X_{\downarrow}^n]$ for the n'th moment of the population frequency after τ units of genetic drift *forwards* in time conditional on population frequency p and $E[X_{\uparrow}^n]$ for the n'th moment of the population frequency going back τ units of genetic drift conditional on population frequency p. These moments are derived below.

Moments for $X_{\downarrow}$

To derive the moments of $X_{\downarrow}$, note that given a population frequency x of the derived variant, the probability of obtaining a sample of size n with only the derived allele is x^n. Thus, $X_{\downarrow}^n$ is the probability to pick only the derived variant in a sample of size n, and $E[X_{\downarrow}^n]$ is the expected value of this probability. Conditional on the frequency of the derived variant being p, τ time units ago, the expected probability for such a sample is derived by averaging over the number of ancestors to the sample τ time units ago, where each of those ancestors need to be of the derived type. Hence, $E[X_{\downarrow}^n|X_0 = p]$, or the expected probability to observe only the derived variant in a sample of size n is

$$E[X_{\downarrow}^n|X_0 = p] = \sum_{k=1}^{n} p^k g_{n,k}(\tau) \tag{3}$$

with $g_{n,k}(\tau)$ being the probability of there being k ancestors at time τ to a sample of n gene-copies (a much longer recursive proof using diffusion theory can be obtained from the authors upon request). Specifically

$$g_{n,k}(\tau) = \frac{1}{\binom{k}{2}} \sum_{i=k}^{n} e^{-\binom{i}{2}\tau} \binom{i}{2} \prod_{l=k, l\neq i}^{n} \frac{\binom{l}{2}}{\binom{l}{2} - \binom{i}{2}} \tag{4}$$

for $2 \leq k < n$ with special cases $g_{n,n}(\tau) = e^{-\binom{n}{2}\tau}$ and $g_{n,1}(\tau) = 1 - \sum_{k=2}^{n} g_{n,k}(\tau)$ (Tavaré, 1984; Wakeley, 2009).

Since $g_{1,1}(\tau) = 1$, $g_{2,2}(\tau) = e^{-\tau}$, $g_{2,1}(\tau) = 1 - e^{-\tau}$ we have

$$
\begin{aligned}
E[X_\downarrow | X_0 = p] &= \sum_{k=1}^{1} p^k g_{1,k}(\tau) = p g_{1,1}(\tau) = p \\
E[X_\downarrow^2 | X_0 = p] &= \sum_{k=1}^{2} p^k g_{2,k}(\tau) = p g_{2,1}(\tau) + p^2 g_{2,2}(\tau) \\
&= p(1 - e^{-\tau}) + p^2 e^{-\tau} = p - e^{-\tau} p(1-p)
\end{aligned}
$$

Moments for $X_\uparrow$

Define $\phi(x, \tau, p)$ to be the probability density of frequency x at time τ, given that $X_A = p$. The density backward in time is, in fact, the same as the forward density conditional on extinction (since by definition the derived variant goes extinct backwards in time) (Griffiths, 2003). The forward density conditional on the allele ultimately going extinct is (using $*$ to denote conditional on extinction)

$$
\phi^*(x, \tau, p) = \phi(x, \tau, p) \frac{u_0(x)}{u_0(p)} \tag{5}
$$

where $u_0(z)$ is the probability of an allele at frequency z ultimately being lost. In a neutral model, $u_0(z) = 1 - z$. We get

$$
\begin{aligned}
E[X_\uparrow^n | X_0 = p] &= \int_0^1 x^n \phi^*(x, \tau, p) dx = \int_0^1 x^n \phi(x, \tau, p) \frac{1-x}{1-p} dx \\
&= \frac{1}{1-p} \left(E[X_\downarrow^n | X_0 = p] - E[X_\downarrow^{n+1} | X_0 = p] \right).
\end{aligned}
$$

For $n = 1$ we have

$$
\begin{aligned}
E[X_\uparrow | X_0 = p] &= \frac{1}{1-p} \left(E[X_\downarrow | X_0 = p] - E[X_\downarrow^2 | X_0 = p] \right) \\
&= \frac{1}{1-p} \left(p - p + e^{-\tau} p(1-p) \right) = e^{-\tau} p
\end{aligned}
$$

How to measure continuity

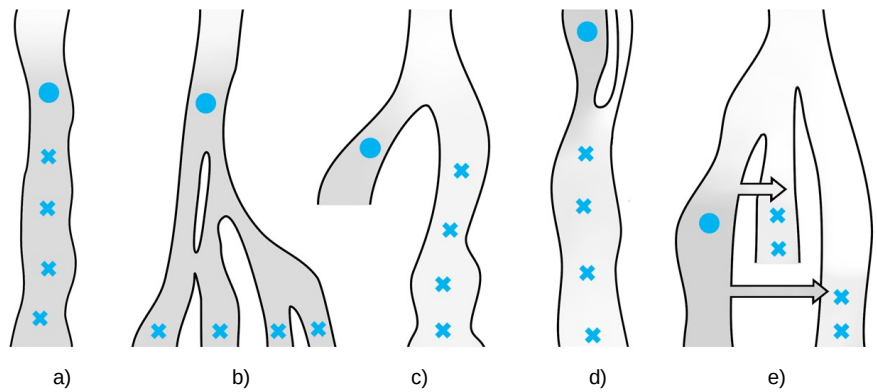

Figure 10: a)-d): scenarios under which all test individuals (blue crosses) are expected to have the same proportion of derived alleles at polymorphic sites in the anchor (blue filled circle). e): although it will depend on the details of the two admixture events (the arrows), this scenario can result in all test individuals (blue crosses) having the same expected proportion of derived alleles at polymorphic sites in the anchor. In all scenarios, the darker the grey, the higher the expected proportion of derived alleles at polymorphic sites in the anchor.

Here we will refer to an individual x being completely continuous with a population A if population A contributed 100% to x in the sense that all ancestors to x that were contemporaneous with population A also belonged to population A. By extension, we will talk about a continuity (or contribution) level of γ from a population A to an individual x meaning that a proportion γ of the genetic material in the genome of x can be traced backwards in time to an individual belonging to population A. Thus, referring to figure 10, we would say that all test individuals are 100% continuous with the anchor population in scenarios a) and b) but 0% continuous for scenario c). For scenario d) γ is somewhere between 0% and 100% and, in scenario e), there is no contribution from the anchor population to the test individuals in the middle (inner) branch, but some level $\gamma > 0$ for the test individuals in the right branch.

In an alternative perspective, we will define the β-drift of test individual x relative to an anchor A as the average amount of backwards drift *from* the anchor population to the population x was sampled from. If a test individual is drawn from the same population as the anchor, the probability to draw the ancestral variant is $\overline{p_A}$ among the chosen set H_A of polymorphic sites in the anchor A. On the other hand, if the average path from the anchor population to

a test individual involves going backwards τ units of genetic drift, the probability to draw the ancestral variant in the population the test individual belongs to is $e^{-\tau}\overline{p_A}$. Thus, we would say that this individual has β-drift$= \tau$. Note here that β-drift$= 0$ implies a contribution at $\gamma = 100\%$ and vice versa. In figure 10, scenarios a) and b) correspond to β-drift 0 from the anchor population to any of the test populations while in scenario c) correspond to β-drift > 0 (possibly very close to 0) corresponding to the drift from the anchor population to the most recent ancestral population of both the test individuals and the anchor. In scenario d), if, for instance, the contribution level is assumed to be $\gamma = 80\%$ and the average amount of backwards drift from the anchor population, via the right branch, back to the test populations is 0.7, the β-drift will be $-ln(0.8 \times 0 + 0.2 \times e^{-0.7})$. In scenario e), the β-drift for the test individuals in the middle branch compared to the β-drift for the test individuals in the right branch will depend on the amount of gene flow in the two admixture events as well as the amount of drift between the anchor and the older admixture event.

The reason for considering both these measures of deviation from perfect continuity is that while continuity at level γ may be closer to the intuitive understanding of deviation from continuity, it is not as practical as the β-drift measure. Consider for example scenario c) in figure 10 when there is almost no drift between the anchor population and the population split. Scenario c) is then (almost) identical to scenario a) although, by definition, the level of continuity is still $\gamma = 0$. The β-drift is however (almost) identical in scenario a) and scenario c) in this case. Because of such considerations, we argue that β-drift is the more useful measure when assessing proximity to (perfect) continuity. Moreover, variation in β-drift in a set of test individuals is exactly mirrored in the variation for the probability to pick the derived variant (in the set of heterozygous anchor sites) among these test individuals. More precisely, because β-drift $= \tau$ implies that the probability to pick the derived variant is $e^{-\tau}\overline{p_A}$, the ratio of the probability to pick the derived variant for an individual with β-drift τ_1 and an individual with β-drift τ_2 is simply $e^{-\tau_1}/e^{-\tau_2}$.

Sample metadata

Table 1: Information on the 10 individuals used in this study. mt, mitochondrial; cal, calibrated; BCE, before common era; PWC, Pitted Ware Culture; TRB, Funnel Beaker Culture.

Sample	Context	Origin	Genome coverage	Contamination (%)		Source	Age (cal. years BCE)	Genetic sex
				mt	autosomal			
sf12	Mesolithic	Stora Förvar, Stora Karlsö	62.16	0.015	0.73	(Günther et al., 2018)	7083-6807	XX
ajv36	PWC	Ajvide, Gotland	10.96	0.029	0.69	(Coutinho et al., 2020)	3200-2300*	XX
ajv49	PWC	Ajvide, Gotland	20.26	0.049	0.66	Unpublished	3200-2300*	XY
ajv54	PWC	Ajvide, Gotland	17.83	0.024	0.47	(Malmström et al., 2019)	3200-2300*	XY
ajv58	PWC	Ajvide, Gotland	17.21	0.045	0.53	(Skoglund et al., 2014a)	2950-2650	XY
ajv82	PWC	Ajvide, Gotland	20.88	0.185	0.65	(Wallin and Martinsson-Wallin, 2016)	3200-2300*	XY
gok18	TRB	Gökhem, Västergötland	14.64	0.089	0.75	(Paulsson, 2010)	3760-3340†	XY
gok21	TRB	Gökhem, Västergötland	13.14	0.158	1.11	(Paulsson, 2010)	3760-3340†	XY
gok22	TRB	Gökhem, Västergötland	13.90	0.205	1.07	(Paulsson, 2010)	3760-3340†	XY
ros16	TRB	Rössberga, Västergötland	19.53	0.065	0.62	(Blank, Sjögren, and Storå, 2020)	3082-2894	XX

* Radiocarbon dates corrected for marine-reservoir effect
† Archaeological context-dated (Paulsson, 2010)

Anchor statistic, *f*-statistics and *D* statistics

Calculation of anchor statistics were performed using custom python scripts and functions. The python program scikit-allel (Miles, A. and Murillo, R. and Ralph, P. and Harding, N and Pisupati, R. and Rae, S. and Millar, T., 2010) was used to calculate *f*2-statistics and *D* statistics (also called the "ABBA-BABA" test (Patterson et al., 2012)). Standard errors for all statistics were calculated using weighted-block jackknife.

ABBA-BABA results

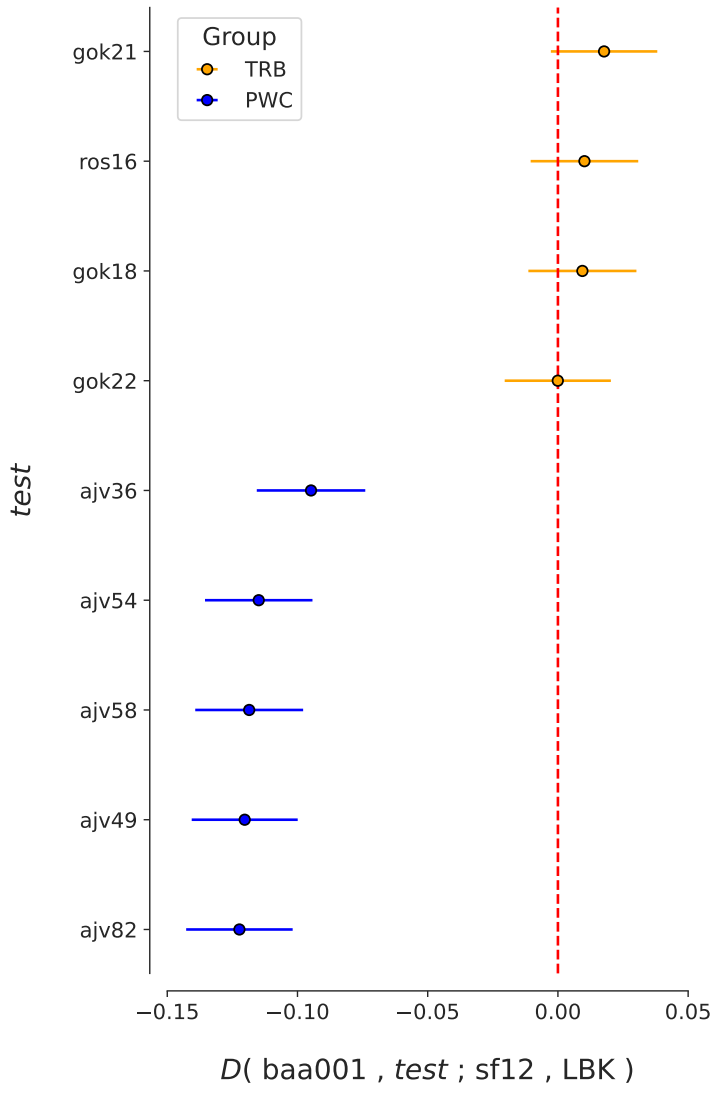

Figure 11: Plot showing results of normalised four-population test for admixture ("ABBA BABA" test) of form D(BallitoBayBoy, *test* ; sf12, LBK).

Downsampling

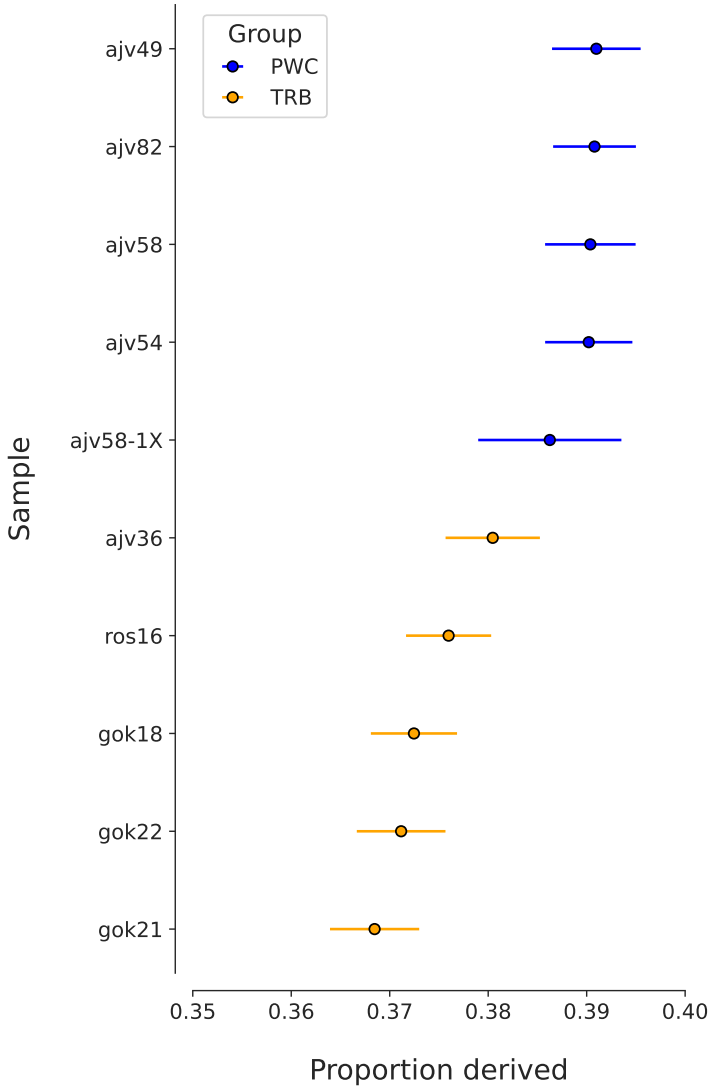

Figure 12: Results of anchor test with ancient individuals from PWC and TRB cultures, including PWC individual ajv58 of mean autosomal coverage $\sim$ 17X downsampled to $\sim$ 1X (ajv58-1X).

BallitoBayBoy as anchor

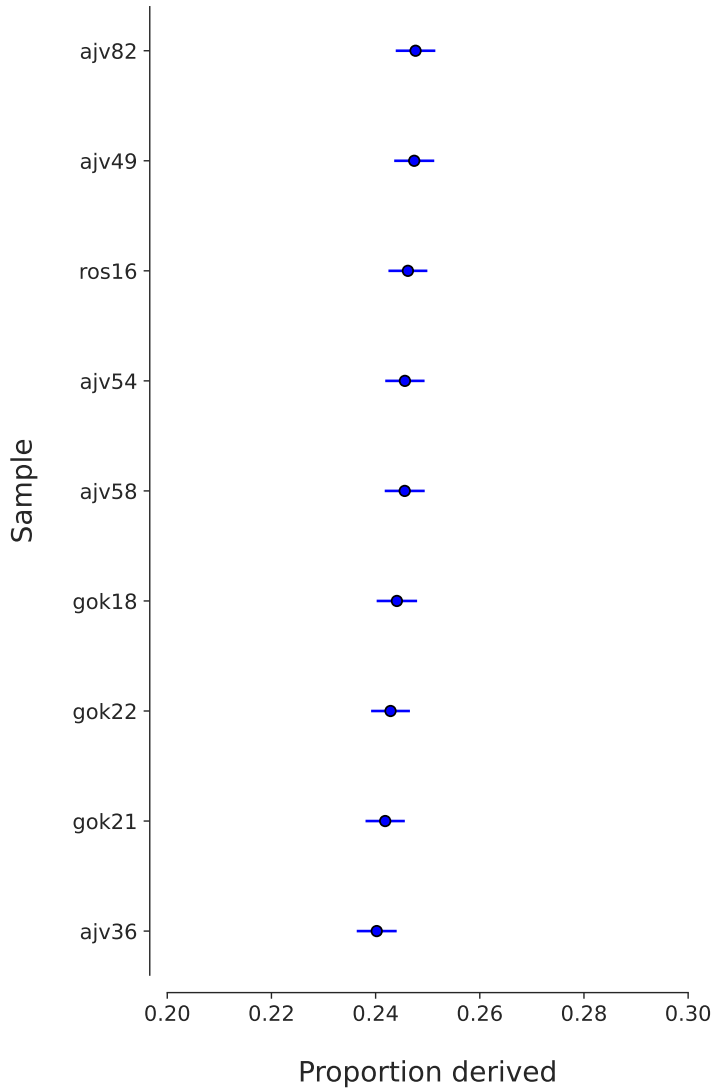

Figure 13: Results of anchor test with ancient individuals, using ancient African hunter gatherer individual BallitoBayBoy (Schlebusch et al., 2017) as anchor.